15 Apr 2004, 1:00pm - 2:45pm

Static and Dynamic Response Analysis of a High Rock-Fill Dam with a Clay Core

Gang Wang
Tsinghua University, Beijing, China

Bing-Yin Zhang
Tsinghua University, Beijing, China

Jian-Min Zhang
Tsinghua University, Beijing, China

Proceedings: Fifth International Conference on Case Histories in Geotechnical Engineering
New York, NY, April 13-17, 2004

STATIC AND DYNAMIC RESPONSE ANALYSIS OF A HIGH ROCK-FILL DAM WITH A CLAY CORE

Gang WANG
Tsinghua University
Beijing 100084, China

Bing-Yin ZHANG
Tsinghua University
Beijing 100084, China

Jian-Min ZHANG
Tsinghua University
Beijing 100084, China

ABSTRACT

Stress strain analysis based on Biot's consolidation theory is performed for Nuozhadu dam, which is a high rock-fill clay-core dam located in the Langcangjiang River in Yunnan province, China. Attention is mainly focused on arching effect and possibility of hydraulic fracturing of the core. Equivalent linear approach is employed to evaluate the seismic response of the dam under design earthquakes, and two empirical formulas relating residual shear and volumetric strain to cyclic stress and strain history are proposed to evaluate the permanent deformation. It is found that: 1) the modulus ratio of the clay in the core to rockfills around is the main factor controlling the severity of arching effect, 2) hydraulic fracture would not occur according to the criterion of effective stress, and 3) the permanent deformation that is likely to occur is acceptable under the condition of design earthquakes.

INTRODUCTION

Nuozhadu hydropower station is a huge water control project at the middle and lower reaches of the Lancangjiang River, 350 km south west of Kunmin in Yunnan Province, China, and 400 km north of the frontier line between China and Thailand. It has a catchment area of 144,700 km^2. The reservoir provides a total storage capacity of 22.5 billion m^3. The objectives of the project are mainly power generation, also flood control, water supply and irrigation.

A 261m high rockfill dam with a clay core, which has to bear about 250m water head during operation period, is designed as a main part of the project (Fig. 1). The height of the dam ranks the first in China and the third in the world. Reliable estimation of possible deformation under various situations must be made to instruct the design of the dam outline and selection of the materials to restrict the deformation to acceptable level. The performance of the dam subject to design earthquakes also must be evaluated. It's a challenging job according to current knowledge of geotechnical practice.

The numerical analysis technology was involved since the beginning of the design, and made a great contribution to the decisions of many important issues, such as the outline and the material zone of the dam, and the selection and compaction coefficient of materials. This paper describes one of the 2-D FEM models to illustrate the analysis techniques used.

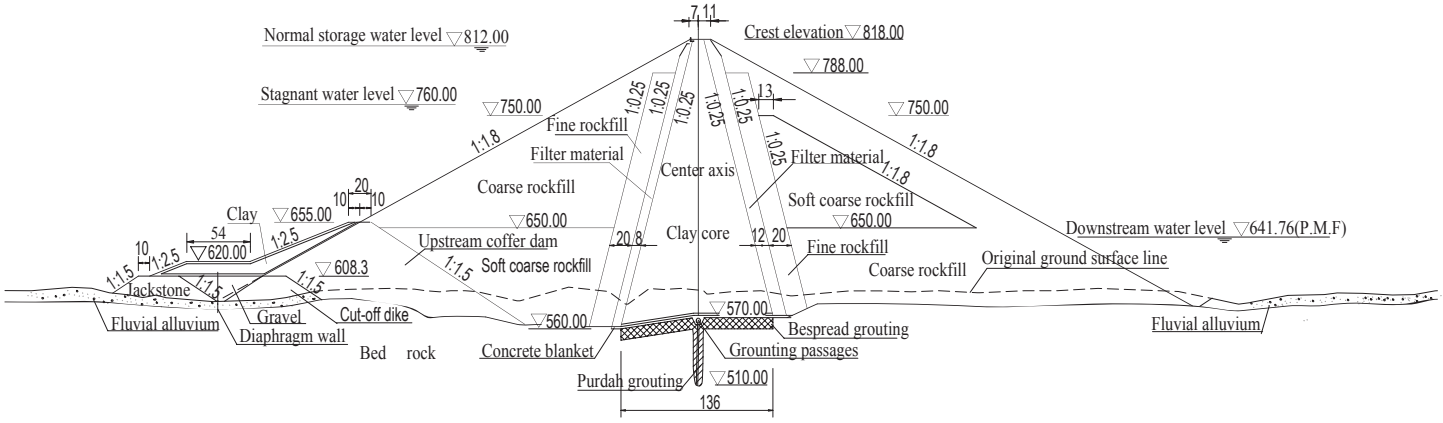

Fig.1. Maximum design section of Nuozhadu rock-fill clay-core dam

Governing Equations

Biot (1941) was the first to develop a general theory for saturated porous media. The matrix-vector form of Biot's consolidation theory was as follows:

$$\begin{cases} [K]\{u\} + [Q]\{p\} = \{f_1\} \\ [Q]^T\{\dot{p}\} + [S]\{\dot{p}\} + [H]\{p\} = \{f_2\} \end{cases} \quad (1)$$

in which, $\{u\}$ is the displacement vector of nodes, $\{p\}$ and $\{\dot{p}\}$ are the pore pressure vector and its change rate respectively, $[K]$ is the stiffness matrix, $[Q]$ and $[Q]^T$ are the discrete gradient operator coupling the solid and fluid phase and its transposition, $[S]$ is the compressibility matrix, $[H]$ is the permeability matrix, $\{f_1\}$ and $\{f_2\}$ are force vectors accounting for prescribed boundary conditions and body force effect for the mixture and the fluid phase respectively.

In the analysis, rockfills are regarded as completely permeable, so only consolidation of clay core is taken into consideration.

Constitutive Model of Soil Skeleton

The deformation behavior of soil is very complex. Even at quite low stress level, it already exhibits nonlinearity and plasticity. Duncan and Chang's *E-B* model (Duncan & Chang, 1970; Duncan et al., 1980) embodies the principle deformation characteristics. It employs two elastic coefficients *E* and *B*, which depend on stress state, to reflect the nonlinearity of soil deformation. It also takes the modulus of unloading and reloading into consideration, so the inelasticity and influences of stress history are partially reflected. Duncan and Chang's *E-B* model was used to represent the stress and strain relationship of soil skeleton in the analysis.

The non-linear *E-B* model is a modified elastic model based on Hook's law expressed in incremental form. The tangent Young's modulus is assumed to be

$$E_t = KP_a\left(\frac{\sigma_3}{p_a}\right)^n (1 - R_f S_l)^2 \quad (2)$$

where S_l is the mobilized shear stress level, determined by

$$S_l = \frac{(1-\sin\phi)(\sigma_1 - \sigma_3)}{2c\cdot\cos\phi + 2\sigma_3\cdot\sin\phi} \quad (3)$$

in which, σ_1 and σ_3 are major and minor principle stress, R_f is failure ratio, K is a model parameter, n is the exponent determining the rate of variation of the initial tangent modulus with σ_3, p_a is the atmospheric pressure expressed in the same unit as σ_3, c and ϕ are the Mohr-Coulomb shear strength parameters. In order to reflect the decrease of the friction angle ϕ of rockfills with the increase of the confining pressure, following formula to determine ϕ was adopted.

$$\phi = \phi_o - \Delta\phi \lg\left(\sigma_3/p_a\right) \quad (4)$$

Also based on experimental findings, Duncan et al. (1980) suggested that the tangent bulk modulus could be estimated from the confining pressure by following formula:

$$B = K_b p_a \left(\sigma_3/p_a\right)^m \quad (5)$$

in which, K_b is a model parameter, m is the exponent determining the rate of variation of the bulk modulus with confining pressure σ_3.

The variation of the tangent Young's modulus with the confining pressure for unloading and reloading may be represented by

$$E_{ur} = K_{ur} p_a (\sigma_3 / p_a)^n \quad (6)$$

in which, K_{ur} is nominated rebound modulus index, determined by unloading/reloading stress path. A criterion, which can distinguish primary loading and unloading or reloading, is needed. A stress state function is introduced as follows:

$$SS = S_l \cdot (\sigma_3 / p_a)^{1/4} \quad (7)$$

where S_l is the mobilized shear stress level described in equation (3). When *SS* is greater than its maximum value, denoted as $(SS)_{max}$, in the stress history, the load state will be recognized as loading. Otherwise, it is considered to be unloading or reloading, the modulus used is determined by equation (6).

There are eight model parameters in the model, including c, ϕ_o, $\Delta\phi$, K, n, R_f, K_b, m

Compressibility Model of Pore Fluids

In most cases, clay core is nearly saturated, so it is reasonable to regard pore fluids including pore water and air as one compressible fluid, and Darcy's law can be used to govern its motion. The main problem is how to quantify its compressibility. The pore fluid's compressibility can be determined by

$$\beta = n\frac{1 - S_r}{p_w + p_a} \quad (8)$$

where β is compressibility coefficient used to construct the compressibility matrix $[S]$ in equation (1), n is the porosity of the soil, p_w is the pore pressure, p_a is the atmospheric pressure, and S_r is the saturation ratio of the soil, which depends on the pore pressure as follows (Hilf, 1948):

$$S_r = (S_r)_o \frac{p_w + p_a}{p_a + (1 - c_h)(S_r)_o\, p_w} \quad (9)$$

where $(S_r)_0$ is the initial saturation ratio, c_h is Henry's coefficient, which can take the value of 0.02 at 20 ℃. Equation (8) is a simplified version of Fredlund's (Fredlund, 1976).

DYNAMIC RESPONSE ANALYSIS TECHNIQUES

The dynamic response analysis of earth structures and soil sites is based on the technology developed in the 1970s and which represents the very first attempt to carry out nonlinear analysis by equivalent linear procedures (abbreviated as EQL). The early EQL analyses (e.g. Seed et al., 1975) are conducted in terms of total stresses and so the effects of seismically induced pore water pressures are not reflected in the computed stresses and accelerations. Also since the analyses are elastic, they cannot predict the permanent deformation directly. Therefore equivalent linear methods are used only to get the distribution of accelerations and shear stresses in the dam. Semi-empirical methods are used to estimate the permanent deformation and pore water pressures using the acceleration and stress data from the equivalent linear analysis.

Martin et al. (1975) developed a one-dimension effective stress dynamic response analysis technique suitable for level or nearly level ground. Shen (1980) extended the method to two dimensional cases. A modified hyperbolic relationship of the shear modulus attenuation curve and damping ratio curve is used to represent the cyclic stress strain behavior of soil, and two semi-empirical formulas are employed to estimate the permanent volumetric and deviatoric deformation potential of soil elements respectively. The computed deformation potentials are taken as the initial strains and transformed into nodal forces. A static consolidation analysis is performed to get excess pore pressure distribution and deformed configuration just after the EQL analysis step. The technique developed by Shen is illustrated in Fig.2. In order to reflect the effect of the excess pore pressure on the shear modulus, the seismic process is divided into several time steps. In each step, iteration is performed to get a consistent system of shear modulus and cyclic shear strain amplitude just the same as common EQL analysis, as well as permanent deformation or excess pore water pressure is computed using empirical formulas. A static consolidation analysis is also performed to capture the pore water dissipation process in each step. That is to say, in each step an EQL analysis and a static consolidation analysis are performed alternatively. The whole dynamic response process will be gotten step by step as described above. We call this technique "pseudo-effective stress dynamic analysis" to distinguish the true effective stress analysis technique based on dynamic consolidation theory (Biot, 1956a & 1956b; Zienkiewicz et al., 1984).

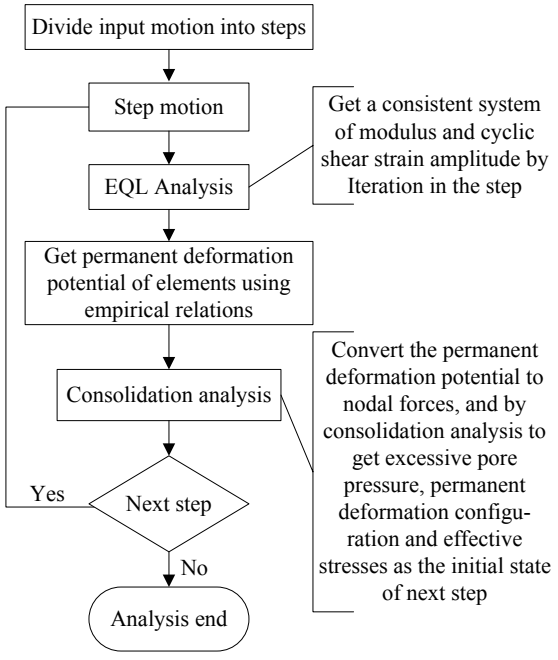

Fig.2 Flow chart of the pseudo-effective stress dynamic response analysis based on EQL procedures

Equivalent Linear Model

Soil subject to symmetric cyclic loading exhibits a hysteresis loop. The hysteresis loop can be described in two ways: first, by the actual path of the loop itself, and second, by parameters that describe its general shape. The equivalent linear model belongs to the latter, and it uses the linear viscoelastic theory to represent the cyclic behavior of soil. In general terms, two important characteristics of the shape of a hysteresis loop are its inclination and its breadth. The inclination of the loop depends on the stiffness of the soil, and the breadth of the loop is an indication of the dissipated energy. The equivalent linear model uses secant shear modulus denoted as G_{sec} and damping ratio denoted as λ to characterize the inclination of the loop and the energy dissipated in a given cycle respectively. G_{sec} and λ vary with cyclic shear strain amplitude in most cases, their different approximation methods bring different models.

The equivalent linear model used here is a revised version of hyperbolic type presented by Hardin and Drnevich (1972). The attenuation relationship of dynamic shear modulus with the shear strain amplitude is expressed by following formula:

$$G_{\mathrm{sec}} = \frac{G_{\max}}{1 + k_1 \gamma_c} \tag{10}$$

where G_{max}, the initial shear modulus, can be estimated by following relation:

$$G_{\max} = k_2 p_a \left(\frac{\sigma'_m}{p_a} \right)^{0.5} \tag{11}$$

k_1,a model parameter, controls the variation rate of the shear modulus with cyclic shear strain amplitude. γ_c, the cyclic shear strain amplitude under uniform strain cycle, depends on the effective pressure and effective cyclic shear strain history.

$$\gamma_c = (\gamma_d)_{eff}^{0.75} \Big/ \left(\frac{\sigma'_m}{p_a} \right)^{\frac{1}{2}} \tag{12}$$

where $(\gamma_d)_{eff}$ is the effective cyclic shear strain, for random strain process it can be selected as $0.65(\gamma_d)_{\max}$ as suggested

by Seed et al. k_2 in equation (11) is also a model parameter which mainly depends on the grain type and void ratio of the soil. σ'_m is the mean effective principal stress.

$$\sigma'_m = \left(\sigma'_1 + \sigma'_2 + \sigma'_3\right)/3 \tag{13}$$

The variation of damping ratio with shear strain is assumed to follow the following formula (Hardin & Drnevich, 1972)

$$\lambda = \lambda_{\max} \frac{k_1 \gamma_c}{1 + k_1 \gamma_c} \tag{14}$$

where $\lambda_{\max}$ is the maximum damping ratio, a material constant.

With Possion's ratio υ assumed as a constant, dynamic bulk modulus can be gotten by following relation

$$K = \frac{2(1+\upsilon)}{3(1-2\upsilon)} G \tag{15}$$

It can be seen that there are four parameters in this equivalent linear model: $k_2, \lambda_{\max}$, k_1, and υ. They can be obtained by fitting modulus reduction curves and damping ratio variation curves.

Permanent Deformation Model

Martin et al. (1975) were the first to present a permanent empirical formula for volumetric deformation under level ground shear. But they cannot give an estimation of the permanent deviatoric strain. Shen et al. (1980 & 1996) gave two formulas for estimating permanent deformation under more general stress states. Two logarithmic functions of the form

$$\varepsilon_{VR} = c_{VR} \ln(1+N) \tag{16}$$

$$\gamma_R = c_{DR} \ln(1+N) \tag{17}$$

were used to fit the accumulation curves of the volumetric and deviatoric strain with the uniform shear strain amplitude cycles N under a given initial static stress state and cyclic shear strain conditions. The curves described by equations (16) and (17) are plotted in Fig.3. The increment formulations are as follows:

$$\Delta\varepsilon_{VR} = c_{VR} \frac{\Delta N}{1+N} \tag{18}$$

$$\Delta\gamma_R = c_{DR} \frac{\Delta N}{1+N} \tag{19}$$

For nonuniform shear strain amplitude sequence, the N is computed as

$$N = \sum \gamma_d \Big/ \overline{\gamma}_d \tag{20}$$

$\overline{\gamma}_d$ is the average shear strain amplitude for a given time period, and $\sum \gamma_d$ is the sum of the shear strain amplitude in the time period.

c_{VR} and c_{DR} control the magnitude of the permanent volumetric and deviatoric strain respectively, which are mainly influenced by the cyclic shear strain amplitude and initial static shear stress level for a given material. The following formulas are used to fit the experimental results:

$$c_{VR} = c_1 \left(\gamma_d\right)_{eff}^{c_2} \exp\left(-c_3 S_l^2\right) \tag{21}$$

$$c_{DR} = c_4 \left(\gamma_d\right)_{eff}^{c_5} S_l^2 \tag{22}$$

in which, S_l is the static mobilized shear stress level, determined by equation (3). This is the key advantage of the presented model compared with the Martin et al.'s model, in the latter, the static shear stress is not considered. Equation (22) shows that the initial static shear stress level has a predominant influence on the permanent deviatoric strain, if the initial shear stress vanished, there would have no permanent deviatoric strain. This is reasonable in common sense.

It has to be pointed out that more and furtherer experiments is needed to verify the effectiveness of the presented model for various materials under various conditions. There are five parameters in the presented model, including c_1, c_2, c_3, c_4, c_5.

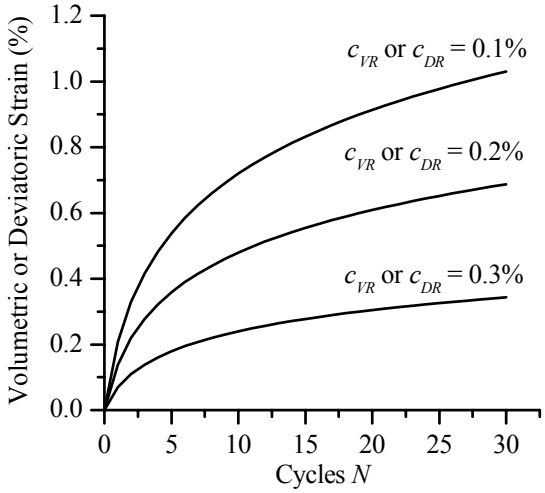

Fig.3 Volumetric and shear strain curves for constant cyclic shear strain amplitude predicted by Eqs.(16) and (17)

FINITE ELEMENT MODEL

The simplified material zone of the dam is schematically illustrated in Fig.4. There are five types of material zones, the material parameters are presented in Table 1, 2 and 3. The parameters for Duncan-Chang *E-B* model are selected based on the results of laboratory triaxial compression tests, while the parameters for dynamic analysis are assumed based on previous practice and experience, and cyclic triaxial tests are under

taking, and will be used in the further analysis. The permeability coefficient of the core material is assumed to be 2.63E-8 m/s, porosity is 0.28, and initial saturation ratio is 0.98. The finite element mesh including construction sequence is illustrated in Fig.5.

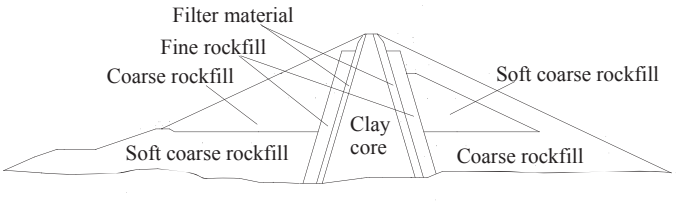

Fig.4 Schematic view of material zones

Fig.6 shows the input ground motion, with a peak value of 2.71 m/s^2, predominant period of 0.2 s and duration of 20 s. The initial stress state before dynamic response analysis is the stress state under the normal storage water level, i.e. ▽812 m.

Table 1. Unit Weight of Materials

Material	γ (10 kN/m^3)	γ_{sat} (10 kN/m^3)
Coarse rockfill	1.995	2.195
Soft coarse rockfill	2.109	2.282
Fine rockfill	2.035	2.213
Filter material	1.958	2.153
Core material	2.156	2.160

Table 2. Duncan-Chang E-B Model Parameters of Materials

Material	ϕ_o (°)	$\Delta\phi$ (°)	R_f	K	n	K_b	m
Coarse rockfill	54.37	10.47	0.719	1491	0.241	683	0.101
Soft coarse rockfill	51.36	9.58	0.706	1400	0.175	474	0.145
Fine rockfill	53.04	8.01	0.632	1300	0.270	650	0.155
Filter material	52.60	10.16	0.761	1100	0.235	340	0.170
Core material	39.47	9.72	0.755	388	0.311	206	0.257

Table 3. Material Parameters for Equivalent Linear Model and Permanent Deformation Model

Material	k_2	$\lambda_{\max}$ (%)	μ	k_1	c_1	c_2	c_3	c_4	c_5
Coarse rockfill	2236	28	0.40	7	0.001	0.75	0	0.20	1
Soft coarse rockfill	2100	28	0.40	7	0.001	0.75	0	0.20	1
Fine rockfill	1950	28	0.40	7	0.001	0.75	0	0.20	1
Filter material	1650	28	0.40	7	0.001	0.75	0	0.20	1
Core material	582	28	0.48	10	0.0012	0.75	1	0.25	1

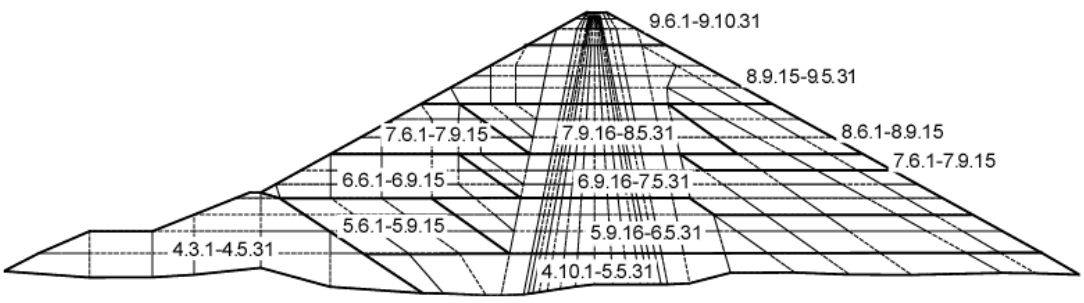

Fig. 5. Finite element mesh and construction sequence (labels in the figure indicate Year.Month.Day)

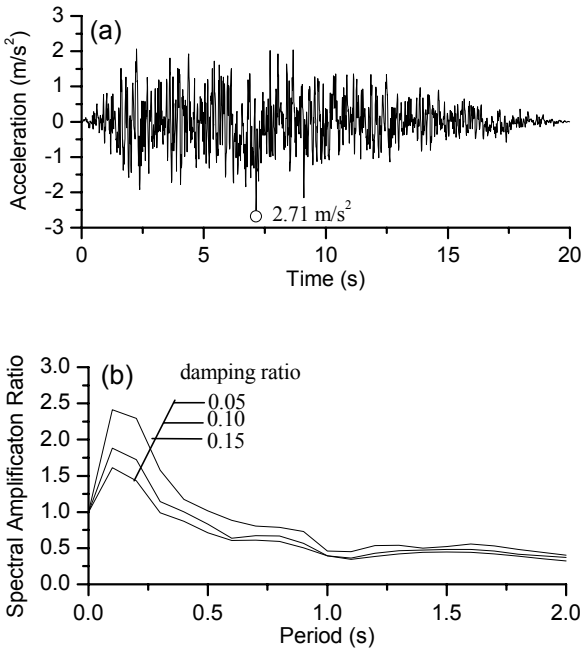

Fig.6. Input motion. (a) Acceleration history, (b) Acceleration response spectra

RESULTS OF STATIC ANALYSIS

The deformation contours of the dam under normal storage water level, i.e. ▽812 m, were given in Fig.7. It can be seen that the maximum horizontal displacement is about 1 m, and maximum settlement is about 3 m.

It's well known that the modulus of the core is much lower than that of rockfills around, so under gravity force a large portion of the stresses of the core will be transferred to adjacent rockfills and cause the stresses of the core much lower than self gravity stresses, this phenomenon is called "arching effect". Arching effect will cause catastrophic consequence such as hydraulic fracture of the core when subject to upstream high water pressure. So much attention would be paid to arching effect of the core especially for such a high dam. The contours of the effective stresses are given in Fig.8. It can be seen that the stresses of the core is much lower than those of rock around at the same elevation. Obviously this means that distinct arching effect has presented itself. The effective stresses of the upstream part of the dam are much lower than those of the downstream part because the pore water pressure in upstream part is much larger than downstream part. The contours of the pore water pressure are plotted in Fig.9, which are almost the same as the static pore water pressure under steady seepage. This shows that the consolidation process of the core under gravity force is almost completed. Although the distinct arching effect exists, the minor principle effective stress in upstream side of the core is well above zero. According to the research of Sun (1985) and Shen et al. (1994), the following criterion was adopted as the necessary condition of hydraulic fracture:

$$\sigma'_{3,\min} + \sigma_t \leq 0 \tag{23}$$

where $\sigma'_{3,\min}$ is the minimum minor principle effective stress , σ_t is the tensile strength of the soil. This criterion indicates that the hydraulic fracture is a type of tension failure. Under the conditions given above, the hydraulic fracture would not occur.

Sensitive analysis has been performed by varying the modulus of the core and rockfills around. It's found that the modulus ratio of the clay in the core to rockfills around was the main factor controlling the severity of arching effect. Proper consideration on the selection of core materials and rolling index has been taken to restrict the possible deformation of the dam and arching effect to an acceptable level.

Fig.10 shows that there is a large area of the upstream part with the mobilized shear stress level S_l close to 1.0. Because the dam deforms toward downstream, the area becomes an active soil wedge. It has no influence on the dam's stability. The stability analysis based on slip slice limit equilibrium method has been performed to insure a safety design of the dam slope.

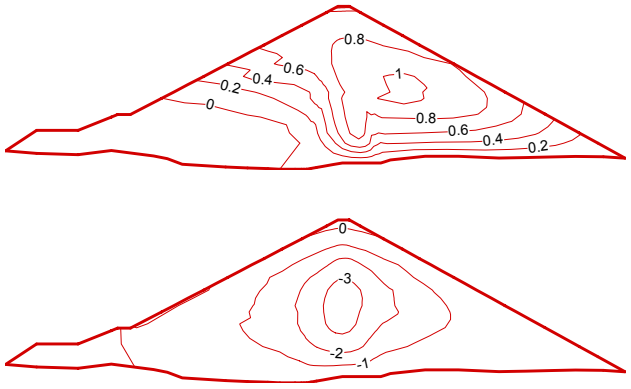

Fig. 7. Deformation contours (m). (a) Horizontal direction, (b) Vertical direction

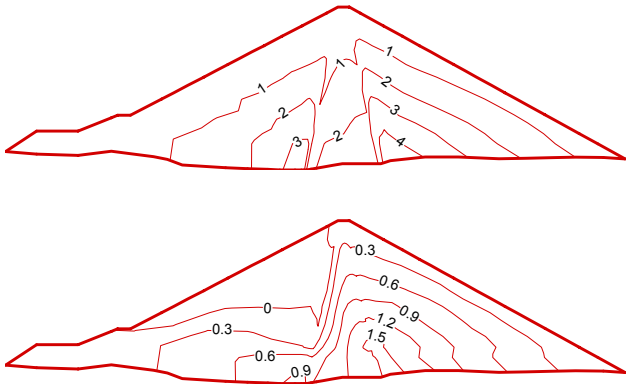

Fig. 8. Effective principal stress contours (MPa). (a) Major principal stress, (b) Minor principal stress

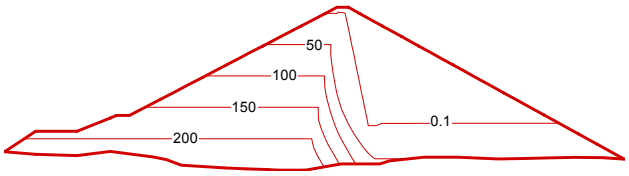

Fig. 9. Pore water pressure contours (m)

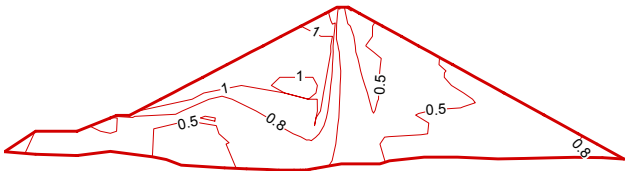

Fig. 10. Mobilized shear stress level contours

RESULTS OF DYNAMIC ANALYSIS

The contours of the maximum acceleration amplification factor of the dam are plotted in Fig.11. The acceleration response inside the dam is not significant mainly because the first natural period of the dam is 1.5 s which is far higher than the predominant period of the input motion 0.2 s. The response acceleration histories of two nodes, located respectively at the top and middle of the dam are given in Fig.12. The curves showing the amplification ratios of transfer functions of these two nodes with periods are given in Fig.13. These curves are computed as the ratios of the response spectral accelerations of the node's motion to those of input motion. It can be seen from Fig.12 that the high frequency components of the input motion are filtered away through the traveling process. Fig.13 shows that the frequency components far away the natural frequencies of the dam are attenuated while those close to the natural frequencies are amplified. The peak acceleration of the crest node is about 3.61 m/s^2.

The contours of the permanent deformation of the dam after earthquake are given in Fig.14. It can be seen that the dam deforms toward downstream, the maximum value is about 0.3 m. This is mainly because that the upstream water level is relatively high (▽812m), and there exists a relatively large static driven shear stress toward downstream. The contours of the permanent settlement show that the settlement of upstream part is much larger than that of the core and downstream part, the deformation concentration was occurred at the interface between the core and upstream part. It can be deduced that local fracture would occur at this area when subject to similar earthquakes.

CONCLUSIONS

The finite element analysis techniques of static stress strain

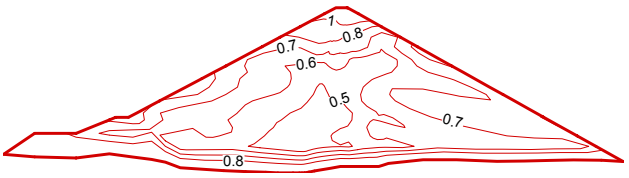

Fig. 11.Contours of maximum acceleration amplification factor in time history

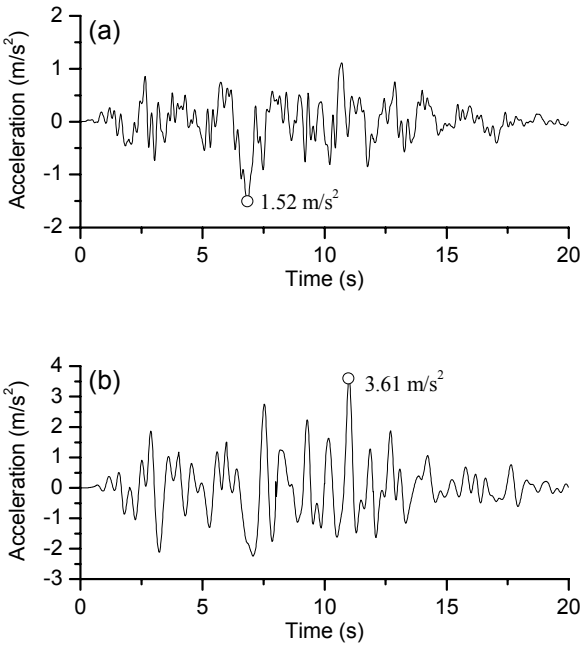

Fig. 12. Response acceleration history of nodes. (a) node at the middle, (b) node at the top

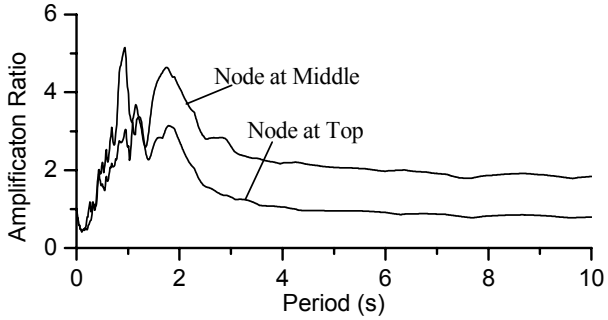

Fig. 13. Transfer functions at two nodes to input motion.(Computed as the ratios of the response spectral accelerations of the node's motion to those of input motion)

analysis and dynamic response analysis performed on the dam of Nuozhadu hydropower station are described through a 2-D FEM model. The following conclusions can be drawn from the analysis.

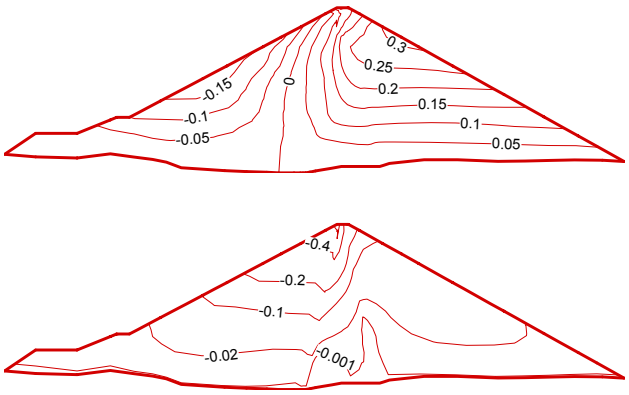

Fig. 14. Permanent deformation after earthquake. (a) Horizontal direction, (b) Vertical direction

(1) The maximum horizontal displacement of the dam is about 1m and the maximum settlement is about 3 m under the condition of normal storage water level. The consolidation process of the core under the gravity force is nearly completed because the construction period is relatively long.

(2) Arching effect causes the effective stresses of the core much lower than rockfills around. But the minimum minor principle stress of the core is well above zero under high upstream water level, so that there is enough safety against hydraulic fracture.

(3) The acceleration response of the dam is not significant because the predominant period of the input motion is much lower than the first natural vibration period of the dam. The maximum acceleration occurs at the crest, the peak acceleration at crest is about 3.61 m/s^2 under design earthquakes.

(4) The permanent settlement of the dam is about 0.5 m, and the maximum horizontal deformation of the dam is about 0.3 m. A large differential settlement taking place between the upstream part and the core may lead to a local fracture.

ACKNOWLEDGEMENTS

The authors would like to express their sincere thanks to Professor Z.J. Shen of Tsinghua University for his help and advice during this study. The authors are also grateful to Dr Y.Z Yu, Mr. L.W. Zhang and Mr. P.C. Fu for their valuable comments on this paper.

REFERENCE

Biot, M.A. [1941]. "General Theory of Three-dimensional Consolidation", J. of Appl. Phys., No.12, pp. 155-164.

Biot, M.A. [1956a]. "Theory of Propagation of Elastic Waves in a Fluid-saturated Porous Solid, Part I: Low Frequency Range", J. of Acoust. Soc. Am., No.2, pp. 168-178.

Biot, M.A. [1956b]. "Theory of Propagation of Elastic Waves in a Fluid-saturated Porous Solid, Part II: Higher Frequency Range", J. of Acoust. Soc. of Am., No.2, pp. 179-191.

Duncan, J.M. and Chang, C.Y. [1970]. "Non-linear analysis of stresses and strains in soils", J. Soil Mech. and Foundation Div., ASCE, No.5, pp. 1629-1653.

Duncan, J.M., Byrne, P., Wong, K.S., et al. [1980]. "Strength, Stress Strain Bulk Modulus Parameters for Finite Element Analysis of Stresses and Movements in Soil Masses", Report no. UCB/GT/80-01, Berkeley, University of California.

Fredlund, D.G. [1976]. "Density and Compressibility Characteristic of Air-water Mixtures", Canadian Geotechnical Journal.

Hilf, J. [1948]. "Estimating Construction Pore Pressure in Rolled Earth Dams", 2nd Int. Conf. Soil Mechs Found Engg., Vol.3.

Seed, H.B., Idriss I.M. and Lee, K.L. et al. [1975]. "Dynamic Analysis of the Slide in the Lower San Fernando Dam during the Earthquake of February 9, 1971", J. Geotech. Div., ASCE No.9, pp.889-911.

Martin, G.R., Finn, W.D.L. and Seed, H.B. [1975]. "Fundamentals of Liquefaction under Cyclic Loading", J. Geotech. Eng. Div., ASCE, No. GT5, pp. 423-438

Shen, Z.J. [1980]. "Numerical Modeling of Dynamic Seepage in Saturated sand", Journal of Hydraulic Engineering, No.2, pp. 14-21 (in Chinese).

Shen, Z.J. [1985]. "A Equivalent Viscoelastic Model for Liquefaction Induced Deformation in Sand", Proc. Forth Chinese Conf. on Soil Mech. and Foundation Eng., Chinese Architecture Press, Beijing (in Chinese).

Shen, Z.J., Yi, J.D. and Zuo, Y.M. [1994]. "Centrifuge Model Test of Hydraulic Fracture of Earth Dam and its Analysis", Journal of Hydraulic Engineering, No.9, pp. 67-98 (in Chinese).

Shen, Z.J. and Xu, G. [1996]. "Deformation Behavior of Rock Materials under Cyclic Loading", Journal of Nanjing Hydraulic Research Institute, No.2, pp. 143-150 (in Chinese).

Sun, Y.P. [1985]. "Study on Mechanism of Hydraulic Fracture", Ph.D. Thesis, Tsinghua University, Beijing, China (in Chinese).

Hardin B.O. and Drnevich V.P. [1972]. "Shear modulus and damping in soils: design equations and curves", J. Soil Mech. and Foundations Div., ASCE, No.SM7, pp. 667-692.

Zienkiewicz, O.C. and Shiomi, T. [1984]. "Dynamic Behaviour of Saturated Porous Media: the Generalized Biot Formulation and its Numerical Solution", Int. J. of Numer. Anal. Meth. Geomechs, pp. 71-96.